PROCEEDINGS of the
23rd International Congress on Acoustics

9 to 13 September 2019 in Aachen, Germany

# Analytical modelling of a MEMS transducer composed of a rigid micro-beam attached at one end to a flat spring moving against a reduced-size backplate

Petr HONZÍK(1), Antonín NOVÁK(2), Stéphane DURAND(2), Nicolas JOLY(2), Michel BRUNEAU(2)

(1)Czech Technical University in Prague, Faculty of Transportation Sciences, Konviktská 20, 110 00 Praha 1, Czech Republic, honzikp@fd.cvut.cz

(2)Laboratoire d'Acoustique de l'Université du Mans (LAUM, UMR CNRS 6613), avenue Olivier Messsiaen 72085, Le Mans, France, antonin.novak@univ-lemans.fr, nicolas.joly@univ-lemans.fr, stephane.durand@univ-lemans.fr, michel.bruneau@univ-lemans.fr

**Abstract**

The use of planar micro-beams as moving parts of acoustic and electroacoustic devices has increased recently because of their geometrical simplicity, hence lowering fabrication costs. The precise modelling of such devices is then of interest. The miniaturized transducer proposed herein is composed of a planar rigid micro-beam attached at one end to a flat spring (the other end remaining free) surrounded by thin slits and loaded by a thin fluid layer (situated in the gap between the micro-beam and a reduced-size backplate) and a small cavity, both being placed behind the beam. Such a configuration reduces the overall size of the device (no need of an external cavity) and enables to adjust more parameters comparing to the case of the backplate of the same size as the one of the micro-beam. The thermoviscous damping effects originating in the fluid-filled parts of the device (slits, air-gap, and cavity) are taken into account. As a result of the model, the displacement of the micro-beam is calculated and compared with the reference finite element solution, the acoustic pressure sensitivity of the transducer is finally presented and discussed.

Keywords: MEMS transducer, micro-beam, analytical modelling

## 1 INTRODUCTION

Precise models of the transducers, particularly of the miniaturized ones, are of interest when an optimization is needed. Such models of the devices containing the micro-beams are of rising importance while some realizations of such transducers has appeared recently [1].

Herein the reduced-size backplate has been employed because of its advantages in terms of sensitivity and bandwidth of the transducer [2]. Since the model of the behaviour of the rigid beam attached at one end to a flat spring loaded by a thin fluid film of uniform thickness [3] and the model of elastically supported rigid beam loaded by fluid film with discontinuity in thickness [4] have been published recently, it is logical to combine herein both approaches together.

Note that in such models the damping originating in the thermal and viscous boundary layers present in the thin airgap and in the slits has to be taken into account [5, 6, 7, 8, 9] along with the coupling between the incident acoustic pressure and the acoustic pressure field inside the transducer through the slits [3, 4].

## 2 ANALYTICAL SOLUTION

The system considered herein is shown in figure 1. The planar rigid micro-beam of length $L$, width $b$ and thickness $h_b$ is attached at the left side to a deformable support acting as a spring (the right side remaining free). The acoustic system surrounding the micro-beam consists of a thin airgap of thickness $h_g$ opened into a small cavity of volume $V_c$ (both being placed behind the micro-beam) and two thin lateral slits of thickness $h_s$ and one thin slit of thickness $h_L$ at the right end of the micro-beam (at $x = L$) coupling the acoustic pressure

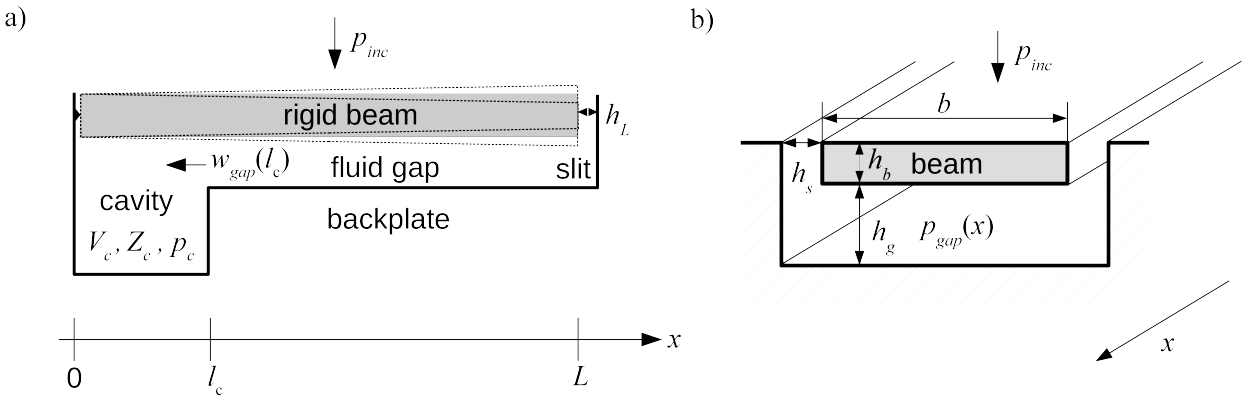


Figure 1. Geometry of the system: a) side view, b) cross-sectional view of the device cut at $x > l_c$

field in all above described acoustic elements with the incident acoustic pressure $p_{inc}$.

### 2.1 The displacement of the beam

The displacement $\eta(x)$ of a planar rigid micro-beam attached at one end to a flat spring is given by the angle $\theta$ through the relation $\eta(x) = \theta x$, the angle being governed by the equation [3]

$$\left[-\omega^2 J + i\omega D_b + C_b\right]\theta = b\int_0^L [p(x) - p_{inc}]\,x\,\mathrm{d}x - 2\int_0^L \left[\frac{dF_{s,y}(x)}{dx}\right] x\,\mathrm{d}x - LF_{L,y}, \tag{1}$$

where $J_b = m_b L^2/3$ is the mass moment of inertia, $m_b$ and $L$ being the mass and the length of the beam respectively, $C_b$ is the force moment and $D_b$ is the damping coefficient of the spring.

### 2.2 The acoustic pressure inside the device

The acoustic pressure $p(x)$ inside the device consists of the pressure field in the airgap $p_{gap}(x)$ and the pressure in the cavity $p_c$ which is supposed to be uniform

$$p(x) = \begin{cases} p_c & x \in (0, l_c) \\ p_{gap}(x) & x \in (l_c, L). \end{cases} \tag{2}$$

Wave equation governing the acoustic pressure field in the thin airgap (between $x = l_c$ and $x = L$) loading the micro-beam is given as follows [3, 4]

$$\left(\frac{\partial^2}{\partial^2 x} + \chi^2\right) p_{gap}(x) = -\left[U_1 p_{inc} + U_2 \eta(x)\right], \tag{3}$$

where $\eta(x)$ is the displacement of the beam, $p_{inc}$ being the incident pressure, the other parameters such as the complex wavenumber $\chi$ and the coefficients on the right-hand side of the equation (3) $U_1$ and $U_2$ being taken from the literature [3].

The solution of the equation (3) takes the classical form

$$p_{gap}(x) = A\cos(\chi x) + B\sin(\chi x) - \frac{1}{\chi^2}(U_1 p_{inc} + U_2 \theta x). \tag{4}$$

The acoustic pressure in the cavity $p_c = w_{tot} Z_c$ is given by the impedance of the cavity $Z_c = \rho_0 c_0^2/(i\omega V_c)$ ($i$ being the imaginary unit, $\omega$ representing the angular velocity, $\rho_0$ and $c_0$ denoting the air density and the

adiabatic speed of sound respectively) and the total volume velocity entering to the cavity

$$w_{tot} = -i\omega b \int_0^{l_c} \eta(x)\mathrm{d}x - w_{gap}(l_c) - 2h_s \int_0^{l_c} \bar{v}_{s,y}(x)\mathrm{d}x \tag{5}$$

which consists of the volume velocity of the beam in the interval $x \in (0, l_c)$, the volume velocity entering from the airgap $w_{gap}(x) = -\partial_x p_{gap}(x) F_{v,g} h_g b/(i\omega\rho_0)$, and the volume velocity entering through the lateral slits [3]

$$\bar{v}_{s,y}(x) = -\frac{1}{i\omega\rho_0}\frac{p_{inc} - p(x)}{h_b} F_{v,s} + \frac{1}{2} i\omega\eta(x) K_{v,s}, \tag{6}$$

where $p(x) = p_c$ in the interval $x \in (0, l_c)$. Reporting the solution for the pressure in the airgap (4) to the expression for the volume velocity at the boundary of the airgap $w_{gap}(l_c)$ gives the pressure in the cavity

$$p_c = \frac{Z_c}{1 + C_1 l_c Z_c}\left[C_1 l_c p_{inc} - (C_2 l_c^2 + C_3 U_2/\chi^2)\theta + C_3(B\chi\cos(\chi l_c) - A\chi\sin(\chi l_c))\right], \tag{7}$$

where

$$\begin{aligned} C_1 &= \frac{2h_s F_{v,s}}{i\omega\rho_0 h_b}, \\ C_2 &= i\omega(b + K_{v,s} h_s)/2, \\ C_3 &= \frac{F_{v,g} h_g b}{i\omega\rho_0}. \end{aligned} \tag{8}$$

The boundary conditions at both sides of the airgap, namely the continuity of between the acoustic pressure in the airgap and in the cavity $p_{gap}(l_c) = p_c$ and the continuity between the volume velocity in the airgap and in the slit at the end of the beam $w_{gap}(L) = \bar{v}_{L,y} h_L b$ (the latter being expressed by the similar way as eq. (6)) enables to express the integration constants of the solution (4)

$$\begin{aligned} A &= \theta H + p_{inc} I, \\ B &= \theta E/D + p_{inc} F/D, \end{aligned} \tag{9}$$

with

$$\begin{aligned} H &= (C_4 + EC_6/D)/C_A, \\ I &= (C_5 + FC_6/D)/C_A, \\ C_4 &= U_2 l_c/\chi^2 - Z_c(C_2 l_c^2 + C_3 U_2/\chi^2)/(1 + Z_c C_1 l_c), \\ C_5 &= U_1/\chi^2 + Z_c C_1 l_c/(1 + Z_c C_1 l_c), \\ C_6 &= -\sin(\chi l_c)) + \cos(\chi l_c) Z_c C_3 \chi/(1 + Z_c C_1 l_c), \\ C_A &= \cos(\chi l_c) + \sin(\chi l_c) Z_c C_3 \chi/(1 + Z_c C_1 l_c), \\ C_7 &= i\omega K_{v,L} h_L b L/2, \\ C_8 &= h_L F_{v,L} b/(i\omega\rho_0 h_b), \\ C_9 &= C_8\cos(\chi L) - C_3\chi\sin(\chi L), \\ D &= -C_3\chi\cos(\chi L) - C_8\sin(\chi L) - C_6 C_9/C_A, \\ E &= C_7 - U_2(C_3 + C_8 L)/\chi^2 + C_4 C_9/C_A, \\ F &= -C_8(1 + U_1/\chi^2) + C_5 C_9/C_A. \end{aligned} \tag{10}$$

The acoustic pressure in the cavity can be finally expressed as

$$p_c = \theta O + p_{inc} P, \tag{11}$$

with

$$\begin{aligned} O &= Z_c\left[EC_3\chi\cos(\chi l_c)/D - HC_3\chi\sin(\chi l_c) - (C_2 l_c^2 + C_3 U_2/\chi^2)\right]/(1 + C_1 l_c Z_c), \\ P &= Z_c\left[FC_3\chi\cos(\chi l_c)/D - IC_3\chi\sin(\chi l_c) + C_1 l_c\right]/(1 + C_1 l_c Z_c). \end{aligned} \tag{12}$$

### 2.3 Coupling between the acoustic pressure and the beam displacement

When reporting the solution for the acoustic pressure inside the transducer into the equation for the displacement of the beam (1), the integral of the pressure in the gap over the airgap length has to be expressed as

$$\int_{l_c}^{L} p_{gap}(x) = \theta J + p_{inc} N \tag{13}$$

with

$$\begin{aligned} J =& HI_C + EI_S/D - U_2(L^3 - l_c^3)/(3\chi^2), \\ N =& II_C + FI_S/D - U_1(L^2 - l_c^2)/(2\chi^2), \\ I_C =& \int_{l_c}^{L} \cos(\chi x) x \ \mathrm{d}x = [\chi L \sin(\chi L) + \cos(\chi L) - \chi l_c \sin(\chi l_c) - \cos(\chi l_c)]/\chi^2, \\ I_S =& \int_{l_c}^{L} \sin(\chi x) x \ \mathrm{d}x = [\sin(\chi L) - \chi L \cos(\chi L) - \sin(\chi l_c) + \chi l_c \cos(\chi l_c)]/\chi^2. \end{aligned} \tag{14}$$

Then, the viscous forces originating in the lateral slits and in the slit at the end of the beam (subscript $s$ and $L$ respectively) are given by [3]

$$\mathrm{d}F_{s,y}(x) = \left[ -\frac{1}{2} K_{v,s} h_s \left( p_{inc} - p(x) \right) + i\omega\eta(x)\Pi_s \right] \mathrm{d}x, \tag{15}$$

$$F_{L,y} = \left[ -\frac{1}{2} K_{v,L} h_L \left( p_{inc} - p(L) \right) + i\omega\eta(L)\Pi_L \right] b, \tag{16}$$

where $\Pi_a = -k_v \mu h_b \cot(k_v h_a)$, the subscript $a$ designates either $s$ or $L$, $\mu$ being the shear dynamic viscosity of the air, and where the pressure at the end of the airgap is

$$p(L) = \theta Q + p_{inc} S, \tag{17}$$

with

$$\begin{aligned} Q =& H\cos(\chi L) + E\sin(\chi L)/D - U_2 L/\chi^2, \\ S =& I\cos(\chi L) + F\sin(\chi L)/D - U_1/\chi^2. \end{aligned} \tag{18}$$

Reporting of the equations (11), (13), (15) and (16) to the equation (1) provides, after some calculation, the final expression for the angle of the beam

$$\theta = p_{inc} \frac{(b - K_{v,s}h_s)(l_c^2 P/2 + N - L^2/2) - K_{v,L} h_L b^2 L(S-1)/2}{-\omega^2 J_b + i\omega D_b + C_b + (l_c^2 O/2 + J)(K_{v,s}h_s - b) + K_{v,L} h_L b^2 L Q/2 + i\omega L^2 (2\Pi_s L/3 + \Pi_L b)}. \tag{19}$$

## 3 RESULTS AND DISCUSSION

In this section the results of the method presented herein are compared with the results of 3D numerical (FEM) simulation obtained using Comsol Multiphysics software [10]. The dimensions of the transducer considered and the properties of the air are given in table 1. The force moment $C_b = 1.0916 \times 10^{-4}$ Nm has been estimated from the numerical simulation of the beam motion without the surrounding acoustic elements, the damping coefficient is neglected $D_b = 0$.

The mean displacement of the beam over the surface of the fixed electrode ($x \in (l_c, L)$), which is the variable of interest when searching for the sensitivity of the electrostatic transducer, given as $\bar{\eta} = \theta(L + l_c)/2$ is shown in figure 2 for the incident acoustic pressure $p_{inc} = 1$Pa. The comparison between the result of the present analytical method (solid line) and the result of the full 3D FEM simulation (black points) shows very good agreement. Given the behaviour of the model near the resonance frequency, the damping in the system seems to be slightly underestimated.

| Parameter | Value | Unit |
|---|---|---|
| Beam length $L$ | $3 \times 10^{-3}$ | m |
| Beam width $b$ | $0.4 \times 10^{-3}$ | m |
| Beam thickness $h_b$ | $50 \times 10^{-6}$ | m |
| Cavity length $l_c$ | $L/4$ | m |
| Cavity thickness $h_c$ | $150 \times 10^{-6}$ | m |
| Airgap thickness $h_g$ | $50 \times 10^{-6}$ | m |
| Thickness of the slits $h_s$ | $10 \times 10^{-6}$ | m |

| Parameter | Value | Unit |
|---|---|---|
| Static pressure $P_0$ | 101330 | Pa |
| Static temperature $T_0$ | 293.15 | K |
| Density $\rho_0$ | 1.204 | kg/m$^3$ |
| Adiabatic speed of sound $c_0$ | 343.2 | m/s |
| Shear dynamic viscosity $\mu$ | $1.814 \times 10^{-5}$ | Pa s |
| Bulk dynamic viscosity $\mu_B$ | $1.088 \times 10^{-5}$ | Pa s |
| Thermal conductivity $\lambda_h$ | $25.77 \times 10^{-3}$ | W/(mK) |
| Ratio of specific heats $\gamma$ | 1.400 | - |
| Specific heat coefficient at constant pressure per unit of mass $C_P$ | 1005 | J/(kgK) |

Table 1. Dimensions of the system and parameters of the thermoviscous fluid (air).

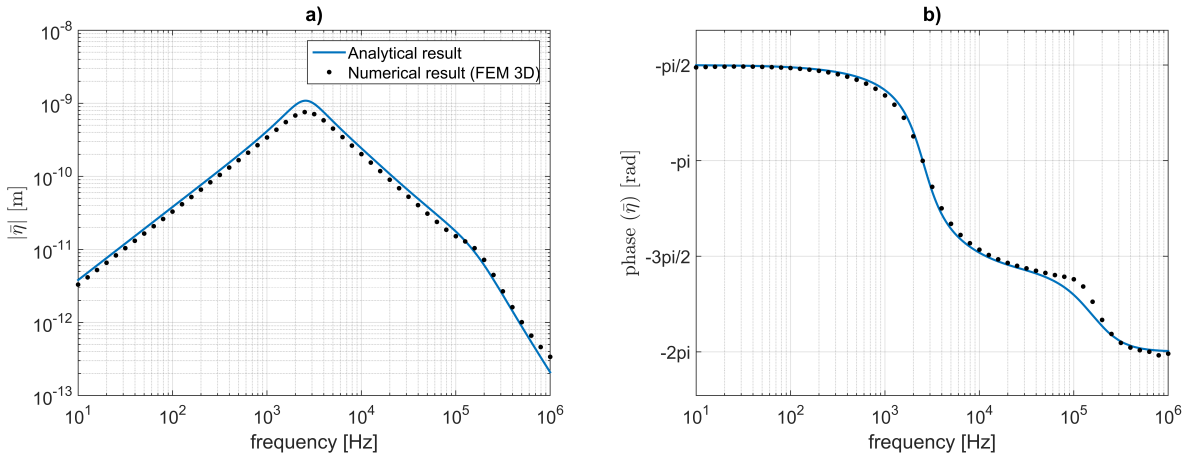


Figure 2. Mean displacement of the beam over the fixed electrode ($x \in (l_c, L)$) calculated analytically (solid line) and using 3D FEM simulation (black points): a) magnitude, b) phase.

In figure 3 the acoustic pressure sensitivity $\sigma = U_0 \bar{\eta} / (p_{inc} h_g)$ of the transducer used as an electrostatic receiver with polarization voltage $U_0 = 30$V is shown. At the left side of the figure the dependence of the sensitivity on the airgap thickness $h_g$ presents very small impact of the variation of this parameter on the frequency response of the transducer. Variation of the thickness of the slits $h_s$ and $h_L$ (right side of the figure) brings, by contrast, an important change in the damping, thus making the frequency response more flat, which is important for MEMS microphones.

## 4 CONCLUSIONS

A simple analytical model of the miniaturized transducer composed of the planar rigid micro-beam attached at one end to a flat spring moving against a reduced-size backplate has been developed. The comparison of the results of the present model and the full 3D numerical (FEM) simulation in terms of the mean displacement of the beam over the reduced-size backplate shows very good agreement, the damping in the system being slightly underestimated. Variation of the thickness of the slits has an important impact on the frequency dependence of the acoustic pressure sensitivity of the transducer used as a receiver, while the impact of the variation of the airgap thickness remains negligible.

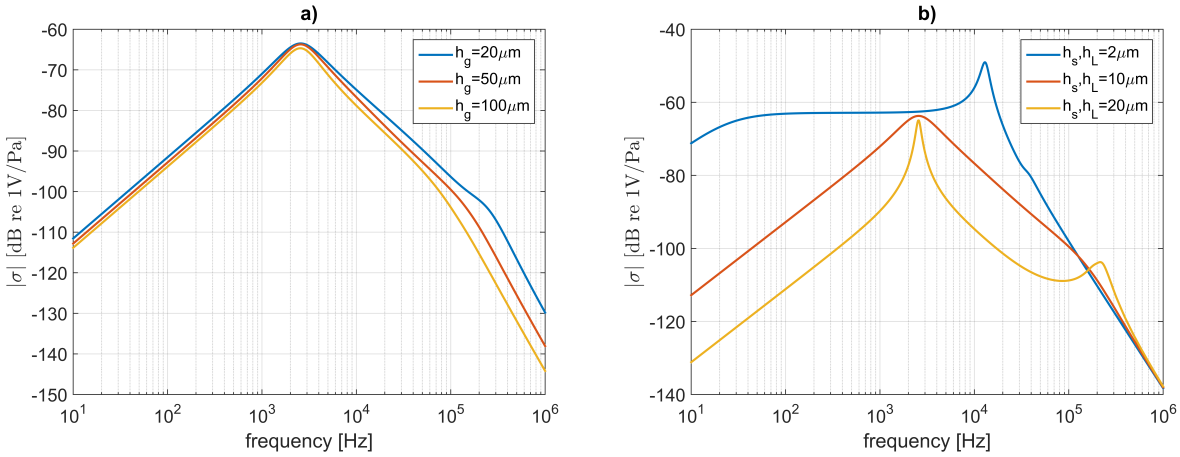


Figure 3. Magnitude of the sensitivity of the transducer for different values a) of the thickness of the airgap $h_g$, b) of the thickness of the slits $h_s$, $h_L$.

## ACKNOWLEDGEMENTS

This work was supported by the Grant Agency of the Czech Technical University in Prague, grant No. SGS18/200/OHK2/3T/16.

## REFERENCES

[1] T. Verdot, E. Redon, K. Ege, J. Czarny, C. Guianvarc'h, J.-L. Guyader, Microphone with planar nano-gauge detection: fluid-structure coupling including thermoviscous effects, Acta Acust. U. Acust. 102(3)(2016), 517 - 529.

[2] P. Honzík, A. Podkovskiy, S. Durand, N. Joly, M. Bruneau, "Analytical and numerical modeling of an axisymmetrical electrostatic transducer with interior geometrical discontinuity", J. Acoust. Soc. Am. **134** (2013), 3573-3579.

[3] A. Novák, P. Honzík, M. Bruneau, "Dynamic behaviour of a planar micro-beam loaded by a fluid-gap: analytical and numerical approach in a high frequency range, benchmark solutions", J. Sound Vib. **401** (2017), 36 - 53.

[4] P. Honzík, A. Novák, S. Durand, N. Joly, M. Bruneau, "Modeling of a one-dimensional acoustic device composed of a planar beam and fluid gap with discontinuity in thickness," Proceeding of Meetings on Acoustics **30** (2017), 030016.

[5] M. Bruneau, A.-M. Bruneau, and P. Dupire, "A Model for Rectangular Miniaturized Microphones", Acta Acustica **3** (1995), 275-282.

[6] P. Honzík, M. Bruneau, "Acoustic fields in thin fluid layers between vibrating walls and rigid boundaries: integral method", Acta Acust. U. Acust. 101(4) (2015), 859 - 862.

[7] T. Veijola, A. Lehtovuori, Numerical and analytical modelling of trapped gas in micromechanical squeeze-film dampers, J. Sound Vib. 319 (1) (2009), 606 - 621.

[8] M. Bruneau, T. Scelo (translator and contributor), *Fundamentals of Acoustics* (ISTE, London, 2006).

[9] M. J. Herring Jensen, E. Sandermann Olsen, "Virtual prototyping of condenser microphone using the finite element method for detailed electric, mechanic, and acoustic characterisation," Proceeding of Meetings on Acoustics **19** (2013), 030039.

[10] COMSOL Multiphysics, User's Guide (2015).